



Adam, M. K., Jarrett-Wilkins, C., Beards, M., Staykov, E., MacFarlane, L. R., Bell, T. D. M., Matthews, J. M., Manners, I., Faul, C. F. J., Moens, P. D. J., Ben, R. N., & Wilkinson, B. L. (2018). 1D Self-Assembly and Ice Recrystallization Inhibition Activity of Antifreeze Glycopeptide-Functionalized Perylene Bisimides. *Chemistry - A European Journal*, 24(31), 7834-7839.  
<https://doi.org/10.1002/chem.201800857>

Peer reviewed version

Link to published version (if available):  
[10.1002/chem.201800857](https://doi.org/10.1002/chem.201800857)

[Link to publication record in Explore Bristol Research](#)  
PDF-document

This is the author accepted manuscript (AAM). The final published version (version of record) is available online via WILEY at <https://onlinelibrary.wiley.com/doi/abs/10.1002/chem.201800857>. Please refer to any applicable terms of use of the publisher.

## University of Bristol - Explore Bristol Research

### General rights

This document is made available in accordance with publisher policies. Please cite only the published version using the reference above. Full terms of use are available:  
<http://www.bristol.ac.uk/red/research-policy/pure/user-guides/ebr-terms/>

# 1D Self-assembly and Ice Recrystallization Inhibition Activity of Antifreeze Glycopeptide-functionalized Perylene bisimides.

Madeleine K. Adam,<sup>[b]</sup> Charles Jarrett-Wilkins,<sup>[c]</sup> Michael Beards,<sup>[d]</sup> Emiliyan Staykov,<sup>[c]</sup> Liam R. MacFarlane,<sup>[c]</sup> Toby D. M. Bell,<sup>[d]</sup> Jacqueline M. Matthews,<sup>[e]</sup> Ian Manners,<sup>[c]</sup> Charl F. J. Faul,<sup>[c]</sup> Pierre D. J. Moens,<sup>[a]</sup> Robert N. Ben<sup>[b]</sup> and Brendan L. Wilkinson<sup>\*[a]</sup>

**Abstract:** Antifreeze glycoproteins (AFGPs) are polymeric natural products that have drawn considerable interest in diverse research fields owing to their potent ice recrystallization inhibition (IRI) activity. Self-assembled materials have emerged as a promising class of biomimetic ice growth inhibitor, yet the development of AFGP-based supramolecular materials that emulate the aggregative behavior of AFGPs have not yet been reported. Here, we demonstrate the first example of the 1D self-assembly and IRI activity of AFGP-functionalized perylene bisimides (AFGP-PBIs). Glycopeptide-functionalized PBIs underwent 1D self-assembly in water and showed modest IRI activity, which could be tuned through substitution of the PBI core. This work presents essential proof-of-principle for the development of novel IRIs as potential supramolecular cryoprotectants and glycoprotein mimics.

Antifreeze glycoproteins (AFGPs) are poly-disperse, mucin-type natural products isolated from deep-sea teleost fish.<sup>[1]</sup> These biological antifreezes exert their physiological function by inhibiting ice growth at sub-zero temperatures, thereby preventing cryoinjury and death.<sup>[2,3]</sup> AFGPs have long drawn interest in diverse fields including cryopreservation, cryosurgery, and food technology owing to their potent ice recrystallization inhibition (IRI) activity.<sup>[4]</sup> The structural and conformational requirements for activity have been intensively investigated, with several studies suggesting a defined polyproline type II helix or an extended

random coil conformation in solution, with different molecular weight fractions possessing variable ice-restructuring properties.<sup>[5]</sup> Solution-phase aggregation and inter-facial absorption of AF(G)Ps have recently been highlighted as important determinants for IRI activity.<sup>[6]</sup> Previous computational studies on type I AFGPs from winter flounder species known to adopt  $\alpha$ -helical structures have also underscored the importance of the hydrophobic domains on the protein for optimizing binding interactions at the ice/water interface.<sup>[7]</sup> The acquisition of AFGPs in sufficient purity and quantity, either from natural sources or total synthesis, is a major practical limitation that has prompted the development of low molecular weight and polymeric mimics.<sup>[8]</sup> The design and synthesis of these molecules has greatly expanded our understanding of AFGP mechanism and yielded some potent IRIs. Supramolecular self-assemblies from low molecular weight building blocks is an emerging and promising strategy for accessing novel IRIs, which has to date included star polymers,<sup>[9]</sup> metallohelices<sup>[10]</sup> and aromatic dye stacks.<sup>[11]</sup> However, the application of bio-functionalized supramolecular structures from the self-assembly of amphipathic AFGP monomers is yet to be reported as a strategy for emulating the aggregative behavior and anti-freeze activity of AF(G)Ps. We postulated that by incorporating planar  $\pi$ -conjugated moieties into AFGP monomers could facilitate 1D self-assembly through  $\pi$ - $\pi$  stacking interactions to provide supramolecular AFGP mimics.

- [a] Dr B. L. Wilkinson, A/Prof P. D. J. Moens  
School of Science and Technology  
University of New England  
Armidale 2351, Australia  
E-mail: Brendan.wilkinson@une.edu.au
- [b] Ms M. K. Adam, A/Prof. Dr. R. N. Ben  
Department of Chemistry and Biomolecular Sciences  
University of Ottawa  
Ottawa K1N 6N5, Canada
- [c] Mr C. Jarrett-Wilkins, Mr L. MacFarlane, Prof. Dr I. Manners, Prof. Dr. C. F. J. Faul  
School of Chemistry  
University of Bristol  
Bristol BS8 1TS, United Kingdom
- [d] Mr. M. Beards, Dr. Toby D. M. Bell  
School of Chemistry  
Monash University  
Melbourne 3800, Australia
- [e] Prof. Dr. J. Matthews,  
School of Life and Environmental Sciences,  
The University of Sydney  
Sydney 2006, Australia

Supporting information for this article is given via a link at the end of the document.

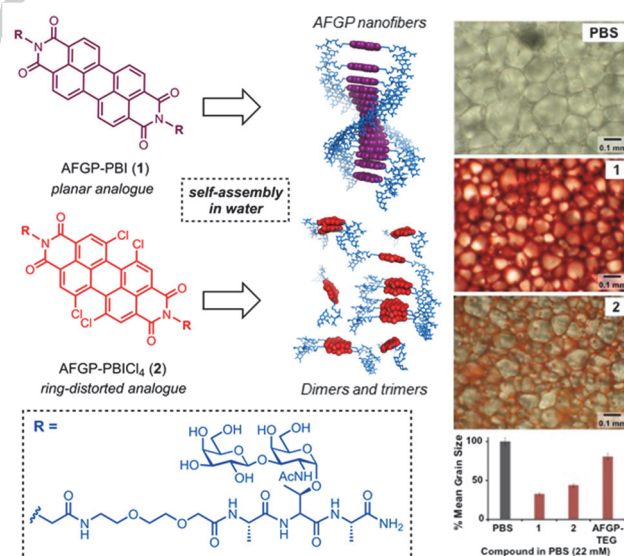


**Figure 1.** Self-assembly and IRI activity of AFGP-PBIs 1 and 2.

Perylene bisimides (PBIs) are a well-studied class of polyaromatic dye that display outstanding fluorescence properties and photo/chemical stability. PBIs have drawn considerable interest as biological probes<sup>[12]</sup> and as supramolecular building blocks for 1D self-assembled materials owing to their strong

propensity to undergo  $\pi$ - $\pi$  stacking in polar and non-polar solvents.<sup>[13]</sup> Water soluble PBIs that incorporate ionic and non-ionic groups in either the bay, ortho or imide position have been actively pursued in bio-sensing and imaging, and as supramolecular materials that mimic biological systems.<sup>[12,14]</sup> The functionalization of the PBI core with chiral, water-solubilizing motifs such as monosaccharides and amino acids is known to give rise to nanoscale structures with programmable helicity and self-assembly properties.<sup>[15]</sup> However, the self-assembly of 1D PBI structures incorporating more complex glycopeptide motifs has never before been reported as a strategy for mimicking functional glycoproteins. In this paper, we describe the 1D self-assembly and ice recrystallization inhibition activity of AFGP-functionalized PBIs (AFGP-PBIs **1** and **2**, Figure 1).

To investigate the effect of core substitution on the self-assembly and IRI activity of these dyes, we targeted two PBIs — AFGP-PBI (**1**) and the bay-substituted tetrachloro- analogue AFGP-PBICl<sub>4</sub> (**2**), to provide a planar and ring-distorted analogue, respectively. We anticipated the structural modification to the PBI core would facilitate variable aggregation properties and thus supramolecular IRI activity. Water-soluble PBIs **1** and **2** were synthesized from adapted literature procedures as described in the ESI.<sup>[16]</sup> A triglycopeptide sequence Ala-Thr-Ala was introduced at the imide position, whereby the Thr hydroxyl group was glycosylated with a  $\beta$ -D-galactosyl-(1,3)-*N*-acetyl- $\alpha$ -D-galactosaminyl disaccharide from the native glycoprotein. A short triethylene glycolate spacer was inserted to promote water solubility and  $\pi$ - $\pi$  stacking interactions between the aromatic faces. In order to investigate the influence of the AFGP side chains and core substitution on the self-assembly properties of these dyes, we examined the steady-state absorption and emission spectra, and performed time-resolved fluorescence measurements. The absorption spectra were acquired at varying concentrations in water and yielded information regarding the electronic coupling of monomers through  $\pi$ - $\pi$  stacking interactions. For the planar PBI **1**, broad unstructured features were observed at concentrations as low as  $5 \times 10^{-6}$  M, with an absorption maxima at 500 nm and a second absorption band at 540 nm (Figure 2a). The loss of vibronic structure corresponding to the unimeric S<sub>0</sub>→S<sub>1</sub> transition became more pronounced at higher concentrations, which was accompanied by a decrease in the molar extinction coefficient. These spectral features, along with a hypsochromic shift in the dominant absorption bands are typical hallmarks of PBI aggregation and suggest the formation of H-type aggregates.<sup>[17]</sup> From the solvent-dependent UV-vis spectra of **1** at  $10^{-4}$  M, the transition from molecularly dissolved species in 3:2 water/acetonitrile to a highly aggregated form in water could be observed (Figure S1). The strong propensity of **1** to aggregate in water is also supported by the fluorescence quantum yield in 3:2 water/acetonitrile at  $5 \times 10^{-6}$  M ( $\Phi = 0.73$ ), which decreased commensurately upon increasing water composition ( $\Phi = 0.07$  in water) (Figure S2 and S3).

Further insight into the self-assembly properties of PBIs **1** and **2** was provided by near UV CD spectroscopy. Since the PBIs incorporate chiral glycopeptide side chains, one would expect a helical bias arising from the transfer of chirality from the side chains to the perylene core of the self-assembled structure.<sup>[18]</sup> For PBI **1** in water, a bisignate Cotton effect was observed with a positive and negative maxima at 500 nm and 450 nm, respectively

(Figure 2c and Figure S4). This signal is consistent with chiral excitonic coupling and the formation of right-handed helical aggregates.<sup>[15d, 19]</sup> The CD signal gradually diminished upon increasing acetonitrile content as the unimeric species predominated. For PBI **2**, a similar bisignate CD signal was seen in water although this signal rapidly diminished upon increasing acetonitrile content, presumably due to the weaker aggregation of this dye (Figure 2d).

From the emission spectra of **1** in water, which provided information relating to the relaxed excimer state, unimeric emission bands at 550 nm and 590 nm were observed at low concentrations ( $5 \times 10^{-8}$  M), which gradually diminished upon increasing concentration (Figure 2b). This was accompanied by an intense red-shifted emission band at 690 nm corresponding to the aggregated state, which increased in intensity upon increasing concentration (up to  $5 \times 10^{-4}$  M).<sup>[14,20]</sup> In order to verify the effect of cooling on aggregation, the excitation and emission spectra of **1** ( $10^{-4}$  M) was also recorded at variable temperature (Figure S5). Encouragingly, no significant change in the spectra was observed upon cooling to 0 °C, thus indicating no significant disaggregation or reorganization of self-assembled structures at lower temperatures. In order to quantify the binding affinity between PBI unimers in water, the dissociation constant ( $K_d$ ) was determined for **1** by measuring the generalized polarization between the assumptively unimeric and aggregated emission bands as a function of concentration (Figure S6).<sup>[21]</sup> Based on this approximation, PBI **1** displayed a  $K_d$  value of  $4.7 \times 10^{-5}$  M, thus indicating a strong driving force for self-assembly in water.

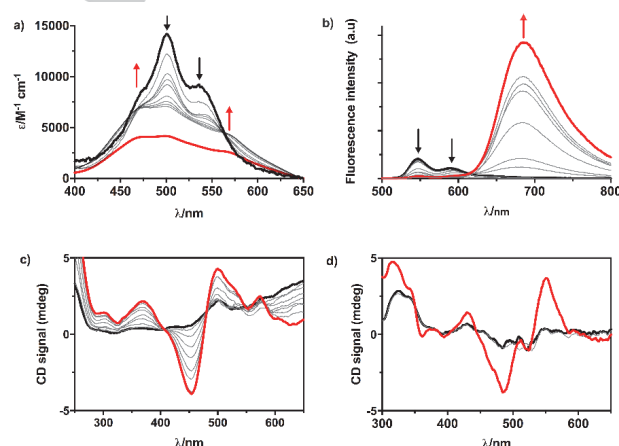


**Figure 2.** a) Concentration dependent UV-vis absorption spectra of PBI **1** in water (solid black:  $c = 5 \times 10^{-6}$  M; solid red:  $c = 5 \times 10^{-4}$  M). b) Fluorescence emission spectra of PBI **1** in water (solid black:  $c = 5 \times 10^{-8}$  M; solid red:  $c = 5 \times 10^{-4}$  M). Arrows indicate the changes upon increasing concentration in water. (c) Solvent-dependent near UV CD spectra of AFGP-PBI **1**, and (d) AFGP-PBICl<sub>4</sub> **2** at  $10^{-4}$  M concentration. Spectra were obtained in water/acetonitrile mixtures at 25 °C (bold red = water, bold black = 40% acetonitrile).

From the UV-vis spectra of **2** in water, a clear vibronic structure was observed across the entire concentration range, thus indicating a preference for unimeric species, which was further supported from solvent-dependent UV-vis studies (Figures S1 and S7). However, a hypsochromic inversion of the dominant absorption bands at 495 nm and 520 nm was seen upon increasing concentration, which provided evidence for weak aggregation in water, presumably through dimer or trimer formation.<sup>[22]</sup> However, from the emission spectra, the emission



band at 550 nm at  $5 \times 10^{-8}$  M did not change considerably upon increasing concentration (up to  $5 \times 10^{-4}$  M), suggesting formation of a non-emissive aggregate (Figure S8). The weak aggregation of **2** was further supported by the fluorescence quantum yield measurements ( $\Phi = 0.94$  in 3:2 water/acetonitrile;  $\Phi = 0.49$  in water) and can be attributed to the twisted perylene core that resulted in impeded  $\pi$ -stacking interactions between the monomers.<sup>[23]</sup> Unfortunately, due to the negligible difference in the excitation and emission spectra for **2** upon increasing concentration, the generalized polarization could not be measured and the  $K_d$  could not be accurately determined. Time-resolved fluorescence studies of **1** and **2** also revealed the lifetime changes upon increasing concentration in water (Figure S9). At a low concentration of **1** ( $5 \times 10^{-6}$  M), a single lifetime could be fitted to the data (5.4 ns). The fractional contribution to this lifetime decreased due to the increasing contribution of a second, shorter lifetime (1.7 ns), which appeared concurrently with the presence of the excimer fluorescence at 690 nm. In contrast, PBI **2** showed only a single fluorescence lifetime of 6.2 ns, which is consistent with weaker aggregation.<sup>[24]</sup> This difference in the aggregation behavior of **1** and **2**, was further confirmed by the anisotropy decay profiles (see ESI).

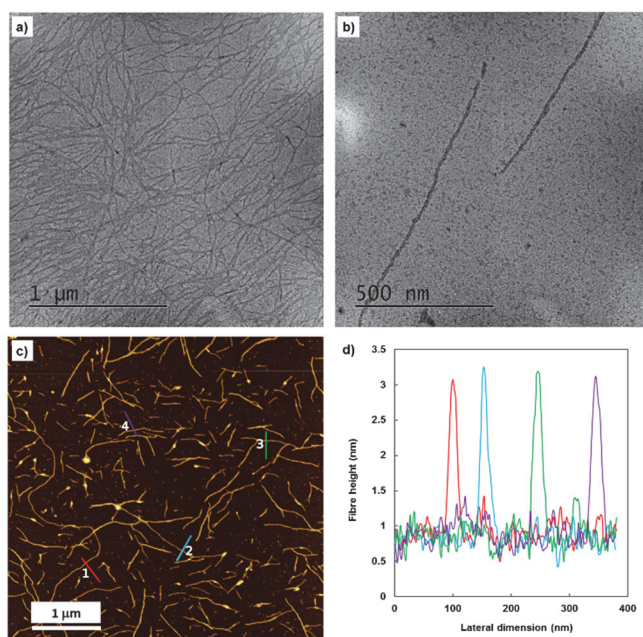


**Figure 3.** a) TEM image of self-assembled nanofibers from **1** ( $c = 10^{-4}$  M). b) Enlarged TEM image of PBI **1** nanofiber from a diluted solution **1** stained with uranyl acetate ( $c = 10^{-5}$  M). c) AFM image of nanofibers from PBI **1** on carbon-coated mica ( $c = 10^{-4}$  M) and d) AFM height profile. N. B. The fibers shown here are not those used for splat-cooling (IRI) assay.

The self-assembled structures from **1** in water were imaged using atomic force microscopy (AFM) and transmission electron microscopy (TEM) (Figure 3). For PBI **1**, one-dimensional fibers were observed by AFM imaging on carbon coated mica, with height profiles of the fibers showing a consistent height of 2.5–3.0 nm. However, no clear evidence for helical aggregates was observed for these glycopeptide nanofibers (Figure S10). Evidence for aggregate formation could be observed by TEM after 1 hour at room temperature, which is in good agreement with spectroscopic studies (Figure S10). In order to determine the effect of cooling on self-assembly of **1**, TEM images were also

acquired at lower variable temperatures after different ageing times (Figure S11). Fibrous morphologies were also observed following sample cooling to  $-16$  °C, which was in good agreement with fluorescence spectroscopic studies.

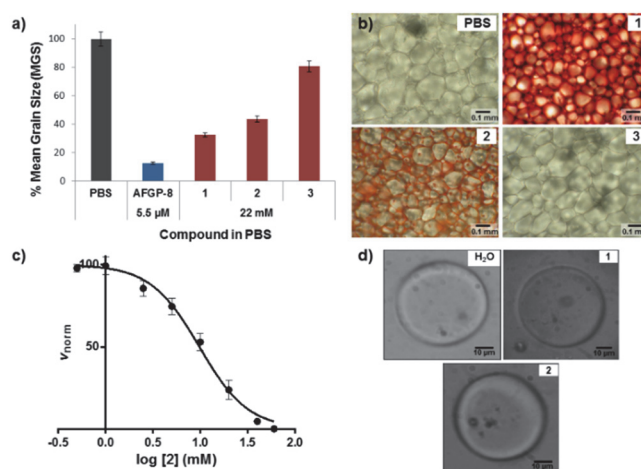


**Figure 4.** a) IRI activity of **1–3** (22 mM) and AFGP8 (5.5  $\mu$ M) in phosphate-buffered saline (PBS) represented as the percent mean grain size (% MGS) of ice crystals relative to the PBS control. Values represent the average of three runs  $\pm$  SEM. b) Ice crystal images of PBS and **1–3** (22 mM) after a 30-minute annealing period at  $-6.4$  °C during the splat-cooling assay. c) Dose-response curve for the IRI activity of **2** ( $IC_{50} = 10$  mM). Normalized rate constants were determined from three experiments  $\pm$  SEM. d) Ice crystal morphology of deionized water, **1** ( $5.0 \times 10^{-4}$  M) in water, and **2** ( $4.6 \times 10^{-3}$  M) in water obtained during nanoliter osmometry.

Having established the aggregation properties of PBIs **1** and **2**, the IRI activity was assessed using a splat-cooling assay (see ESI for details).<sup>[25]</sup> Samples were dissolved in phosphate-buffered saline (22 mM in PBS) and annealed at 90 °C for 1 hour prior to cooling and storage at room temperature for 24 h. To confirm aggregation was occurring prior to the assay, we performed time-dependent fluorescence emission spectroscopy on PBI **1** in PBS buffer ( $c = 1.5 \times 10^{-4}$  M) and measured the ratio of the fluorescence intensity for peaks corresponding to the monomeric (547 nm) and aggregated forms (673 nm) (Figure S12). Encouragingly, no change in this ratio was observed after 10 min of sample preparation (up to 5 h), suggesting aggregation and equilibration had occurred after this time. Both PBIs weakly inhibited ice recrystallization with similar inhibitory potency, with the planar analogue **1** displaying more potent activity compared with the ring-distorted derivative **2** (Figure 4). Notably, the AFGP tripeptide fragment lacking the perylene core (AFGP-TEG, **3**) displayed weaker activity, thus confirming the importance of the hydrophobic PBI core and potentially 1D aggregation for inhibiting ice recrystallization. To probe this further, the IRI activity of PBI **2** was also measured at 10 mM and compared with the glycopeptide **3** at 20 mM (Figure S13). Encouragingly, PBI **2** displayed enhanced IRI activity compared with the tri-glycopeptide control, and whilst the effect is modest, it is significant and strongly suggests the importance of the PBI core and 1D aggregation for activating IRI activity. Unfortunately, in the absence of water-solubilizing appendages, the IRI activity of the PBI core alone could not be assessed, even at very low concentration. The half maximal inhibitory concentration ( $IC_{50}$ ) value of **2** was determined to be 10 mM (Figure 4c and ESI), which, to put into context, is the

same or better than many previously reported amphiphilic C-AFGP analogues bearing a pyranose residue with long alkyl chains.<sup>[26]</sup> Interestingly, unlike AFGP8, a naturally occurring isolate with an average molecular weight of 2.6 kDa, AFGP-PBIs **1** and **2** did not exhibit any thermal hysteresis (TH) or dynamic ice shaping (DIS) properties and thus do not strongly bind to ice. Whilst the IRI activity of the AFGP-PBIs is weak compared with AFGP8, the absence of ice reshaping properties is encouraging since this has been shown to strongly correlate with damaging ice spicule formation at higher concentrations of AFGPs.<sup>[3b, 27]</sup>

In summary, we report the self-assembly and IRI activity of two water-soluble, glycopeptide-functionalized PBIs. The planar PBI **1** underwent 1D self-assembly in water to give extended nanofibers as shown from TEM and AFM imaging, with evidence of helical aggregates from the CD spectra. PBI **1** was shown to be a weak inhibitor of ice recrystallization and unlike the natural glycoprotein, did not exhibit any TH or DIS properties. This suggests that the PBI or its self-assembled structure does not strongly bind to ice, which may be a result of the incorrect spatial presentation of the hydrophobic moieties on the glycopeptide to the ice crystal surface.<sup>[28]</sup> In contrast to **1**, the ring-distorted analogue **2** displayed weak aggregation in water from the absorption and emission spectra, and was shown to be a weaker IRI than **1**. The enhanced IRI activity of these constructs compared with the tri-glycopeptide control, along with the attenuated activity of the ring-distorted analogue **2** relative to **1**, both strongly suggest the importance of 1D self-assembly for activation of IRI activity of low molecular weight AFGPs. Whilst the mechanism for IRI activity of these new PBIs remains to be elucidated, and is weak compared to previously reported polymeric and supramolecular IRIs, this nevertheless represents important proof-of-principle for the future development of biomimetic IRIs presenting native AFGP motifs, along with 1D self-assembled networks presenting bioactive glycopeptides. Future work will focus on determining the mechanism of IRI activity and the lack of ice binding properties using molecular dynamics simulations, along with the development of more potent analogues employing alternative  $\pi$ -conjugated systems.

## Acknowledgements

B. W. would like to thank the Australian Research Council DECRA award (DE130101673) and the University of New England for funding. R. N. B. acknowledges the Natural Sciences and Engineering Research Council of Canada (NSERC), Canadian Blood Services (CBS) and Canadian Institutes of Health Research (CIHR) for financial support. M. K. A. and E. S. would like to thank NSERC for a Canada Graduate Scholarship (CGS D) and Undergraduate Student Research Award (USRA), respectively.

## Conflict of Interest

The authors declare no conflicts of interest.

**Keywords:** 1D self-assembly • perylene bisimides • antifreeze glycopeptides.

- [1] (a) A. L. DeVries, D. E. Wohlschlag, *Science* **1969**, *163*, 1073–1075; (b) A. L. DeVries, S. K. Komatsu, R. E. Feeney, *J. Biol. Chem.* **1970**, *245*, 2901–2908; (c) M. M. Harding, P. I. Anderberg, A. D. J. Haymet, *Eur. J. Biochem.* **2003**, *270*, 1381–1392.
- [2] (a) D. M. Mulvihill, K. F. Geoghegan, Y. Yeh, K. DeRemer, D. T. Osuga, F. C. Ward, R. F. Feeney, *J. Biol. Chem.* **1980**, 659–662; (b) J. A. Raymond, A. L. DeVries, *Proc. Natl. Acad. Sci. USA* **1977**, *74*, 2589–2593; (c) C. A. Knight, C. C. Cheng, A. L. DeVries, *Biophys. J.* **1991**, *59*, 409–418; (d) C. A. Knight, E. Driggers, A. L. DeVries, *Biophys. J.* **1993**, *64*, 252–259; (e) C. A. Knight, A. L. DeVries, *J. Cryst. Growth* **1994**, *143*, 301–310; (f) P. W. Wilson, *Cryo Lett.* **1993**, *14*, 31–36.
- [3] (a) J. A. Raymond, A. L. DeVries, *Proc. Natl. Acad. Sci. USA* **1977**, *74*, 2589–2593; (b) A. D. J. Haymet, L. G. Ward, M. M. Harding, *J. Am. Chem. Soc.* **1999**, *121*, 941–948; (c) N. Pertaya, C. B. Marshall, C. L. DiPrinzio, L. Wilen, E. S. Thomson, J. S. Wettlaufer, P. L. Davies, I. Braslavsky, *Biophys. J.* **2007**, *92*, 3663–3673.
- [4] (a) J. –H. Wang, *Cryobiology*, **2000**, *41*, 1–9; (b) R. E. Feeney, Y. Yeh, *Trends Food Sci. Technol.* **1998**, *9*, 102–106.
- [5] (a) Y. Tachibana, G. L. Fletcher, N. Fujitani, S. Tsuda, K. Monde, S. –I. Nishimura, *Angew. Chem. Int. Ed.* **2004**, *43*, 856–862; (b) V. Bouvet, R. N. Ben, *Cell Biochem Biophys* **2003**, *39*, 133–144; (c) A. N. Lane, L. M. Hays, R. E. Feeney, L. M. Crowe, J. H. Crowe, *Protein Sci.* **1998**, *7*, 1555–1563; (d) A. N. Lane, L. M. Hays, N. Tsvetkova, R. E. Feeney, L. M. Crowe, J. H. Crowe, *Biophys. J.* **2000**, *78*, 3195–3207; (e) B. L. Wilkinson, R. S. Stone, C. J. Capicciotti, M. Thaysen-Andersen, J. M. Matthews, N. H. Packer, R. N. Ben, R. J. Payne, *Angew. Chem. Int. Ed.* **2012**, *51*, 3606–3610; (f) M. Urbańczyk, J. Góra, R. Latajka, N. Sewald, *Amino Acids*, **2017**, 209–222.
- [6] (a) V. Bouvet, G. R. Lorello, R. N. Ben, *Biomacromol.* **2006**, *7*, 565–571; (b) D. Sarno, A. V. Murphy, E. S. DiVirgilio, W. E. Jones Jr., R. N. Ben, *Langmuir* **2003**, *19*, 4740–4744.
- [7] A. Wierzbicki, P. Dalal, T. E. Cheatham, J. E. Knickelbein, A. D. J. Haymet, J. D. Madura, *Biophys. J.* **2007**, *93*, 1442–1451.
- [8] (a) J. Garner, M. M. Harding, *ChemBioChem* **2010**, *11*, 2489–2498; (b) R. Peltier, M. A. Brimble, J. M. Wojnar, D. E. Williams, C. W. Evans, A. L. DeVries, *Chem. Sci.* **2010**, *1*, 538–551; (c) A. K. Balcerzak, C. J. Capicciotti, J. G. Briard, R. N. Ben, *RSC Adv.* **2014**, *4*, 42682–42696; (d) T. Congdon, R. Notman, M. Gibson, *Biomacromol.* **2013**, *14*, 1578–1586; (e) L. L. C. Olijve, M. M. R. M. Hendrix, I. K. Voets, *Macromol. Chem. Phys.* **2016**, *217*, 951–958; (f) C. I. Biggs, T. L. Bailey, B. Graham, C. Stubbs, A. Fayer, M. I. Gibson, *Nat. Commun.* **2017**, *8*, doi:10.1038/s41467-017-01421-7.
- [9] D. J. Phillips, T. R. Congdon, M. I. Gibson, *Polym. Chem.* **2016**, *7*, 1701–1704.
- [10] D. E. Mitchell, G. Clarkson, D. J. Fox, R. A. Vipond, P. Scott, M. I. Gibson, *J. Am. Chem. Soc.* **2017**, *139*, 9835–9838.
- [11] R. Drori, C. Li, C. Hu, P. Raiteri, A. L. Rohl, M. D. Ward, B. Kahr, *J. Am. Chem. Soc.* **2016**, *138*, 13396–13401.
- [12] (a) M. Sun, K. Müllen, M. Yin, *Chem. Soc. Rev.* **2016**, *45*, 1513–1528; (b) T. Weil, M. A. Abdalla, C. J. Hengstler, K. Müllen, *Biomacromol.* **2005**, *5*, 68–79; (c) J. Qu, C. Kohl, M. Potte, K. Müllen, *Angew. Chem. Int. Ed.* **2004**, 1528–1531; (d) S. K. Yang, X. Shi, S. Park, S. Doganay, T. Ha, S. C. Zimmerman, *J. Am. Chem. Soc.* **2011**, *133*, 9964–9967.
- [13] (a) K. R. Wang, H. W. An, R. X. Rong, Z. –R. Cao, X. L. Li, *Macromol. Rapid Commun.* **2014**, *35*, 727–734; (b) Q. Zhao, K. Li, S. Chen, A. Qin, D. Ding, S. Zhang, Y. Liu, B. Liu, J. Z. Sun, *J. Mater. Chem.* **2012**, *22*, 15128–15135; (c) F. Würthner, C. R. Saha-Möller, B. Fimmel, S. Ogi, P. Leowanawat, D. Schmidt, *Chem. Rev.* **2016**, *116*, 962–1052; (d) S. Chen, P. Slattum, C. Wang, L. Zang, *Chem. Rev.* **2015**, *115*, 11967–11998; (e) F. S. Kim, G. Ren, S. A. Jenekhe, *Chem. Mater.* **2011**, *23*, 682–732; (f) C. Huang, S. Barlow, S. R. Marder, *J. Org. Chem.* **2011**, *76*, 2386–2407.
- [14] (a) D. Görl, X. Zhang, F. Würthner, *Angew. Chem. Int. Ed.* **2012**, *51*, 6328–6348; (b) X. Zhang, S. Rehm, M. M. Safont-Sempere, F. Würthner, *Nat. Chem.* **2009**, *1*, 623–629; (c) A. Sorrenti, J. Leira-Iglesias, A. Sato,

- T. Hermans, *Nat. Commun.* **2017**, *8*, doi:10.1038/ncomms15899; (d) Y. Tidhar, H. Weissman, S. G. Wolf, A. Gulino, B. Rybtchinski, *Chem. Eur. J.* **2011**, *17*, 6068–6075.
- [15] (a) J. Hu, W. Kuang, K. Deng, W. Zou, Y. Huang, Z. Wei, C. F. J. Faul, *Adv. Func. Mater.* **2012**, *22*, 4149–4158; (b) X. Liu, Z. Huang, Y. Huang, L. Zhu, J. Fu, *J. Phys. Chem. C* **2017**, *121*, 7558–7563; (c) S. Bai, S. Debnath, N. Javid, P. W. J. M. Frederix, S. Fleming, C. Pappas, R. V. Ulijn, *Langmuir* **2014**, *30*, 7576–7584; (d) G. Echue, G. C. Lloyd-Jones, C. J. Faul, *Chem. Eur. J.* **2015**, *21*, 5118–5128; (e) K. Sun, C. Xiao, C. Liu, W. Fu, Z. Wang, Z. Li, *Langmuir* **2014**, *30*, 11040–11045.
- [16] (a) J. S. Zhao, J. H. Wang, W. B. He, Y. B. Ruan, Y. B. Jiang, *Chem. Eur. J.* **2012**, *18*, 3631–3636; (b) Y. J. Xu, S. W. Leng, C. M. Xue, R. K. Sun, J. Pan, J. Ford, S. Jin, *Angew. Chem. Int. Ed.* **2007**, *46*, 3896–3899; (c) C. Lemouchi, S. Simonov, L. Zorina, C. Gautier, P. Hudhomme, P. Batail, *Org. Biomol. Chem.* **2011**, *9*, 8096–8101.
- [17] (a) Z. Chen, B. Fimmel, F. Würthner, *Org. Biomol. Chem.* **2012**, *10*, 5845–5855; (b) T. Heek, C. Fasting, C. Rest, X. Zhang, F. Würthner, R. Haag, *Chem. Commun.* **2010**, *46*, 1884–1886; (c) D. Sahoo, M. Peterca, M. Aqad, B. E. Partridge, P. A. Heiney, R. Graf, H. W. Spiess, X. Zeng, V. Percec, *J. Am. Chem. Soc.* **2016**, *138*, 14798–14807.
- [18] (a) S. Ghosh, X. –Q. Li, V. Stepanenko, F. Würthner, *Chem. Eur. J.* **2008**, *14*, 11343–11357; (b) M. Liu, L. Zhang, T. Wang, *Chem. Rev.* **2015**, *115*, 7304–7397; (c) C. Roche, H. –J. Sun, P. Leowanawat, F. Araoka, B. E. Partridge, M. Peterca, D. A. Wilson, M. E. Prendergast, P. A. Heiney, R. Graf, H. W. Spiess, X. Zeng, G. Ungar, V. Percec, *Nat. Chem.* **2016**, *8*, 80–89.
- [19] J. van Herrikhuyzen, A. Syamakumari, A. P. H. J. Schenning, E. W. Meijer, *J. Am. Chem. Soc.* **2014**, *126*, 10021–10027.
- [20] Z. Chen, V. Stepanenko, V. Dehm, P. Prins, L. D. A. Siebbeles, J. Seibt, P. Marquetand, V. Engel, F. Würthner, *Chem. Eur. J.* **2007**, *13*, 436–449.
- [21] E. Terpetschnig, H. Szmecinski, J. R. Lakowicz, *Anal. Biochem.* **1995**, *227*, 140–147.
- [22] J. M. Lim, P. Kim, M. –C. Yoon, J. Sung, V. Dehm, Z. Chen, F. Würthner, D. Kim, *Chem. Sci.* **2013**, *4*, 388–397.
- [23] (a) J. Baram, E. Shirman, N. Ben-Shitrit, A. Ustinov, H. Weissman, I. Pinkas, S. G. Wolf, B. Rybtchinski, *J. Am. Chem. Soc.* **2008**, *130*, 14966–14967; (b) D. Görl, X. Zhang, V. Stepanenko, F. Würthner, *Nat. Commun.* **2015**, DOI: 10.1038/ncomms8009; (c) Z. Chen, M. G. Debijie, T. Debaerdemaeker, P. Osswald, F. Würthner, *ChemPhysChem* **2004**, *5*, 137–140; (d) W. Wang, A. D. Shaller, A. D. Q. Li, *J. Am. Chem. Soc.* **2008**, *130*, 8271–8279; (e) K. Bag, P. Kumar Sukul, D. Chandra Santra, A. Roy, S. Malik, *RSC Adv.* **2016**, 34027–34037.
- [24] (a) R. L. Christensen, R. C. Drake, D. Phillips, *J. Phys. Chem.* **1986**, *90*, 5960–5967; (b) R. F. Fink, J. Seibt, V. Engel, M. Renz, M. Kaupp, S. Lochbrunner, H. –M. Zhao, J. Pfister, F. Würthner, B. Engels, *J. Am. Chem. Soc.* **2008**, *130*, 12858–12859.
- [25] C. A. Knight, J. Hallett, A. L. DeVries, *Cryobiology*, **1988**, *25*, 55–60.
- [26] J. F. Trant, R. A. Biggs, C. J. Capicciotti, R. N. Ben, *RSC Adv.* **2013**, *3*, 26005–26009.
- [27] C. Knight, C. Cheng, A. DeVries, *Biophys. J.* **1991**, *59*, 409–418.
- [28] K. Mochizuki, V. Molinero, *J. Am. Chem. Soc.* **2018**, DOI: 10.1021/jacs.7b13630



Layout 1:

## Text for Table of Contents

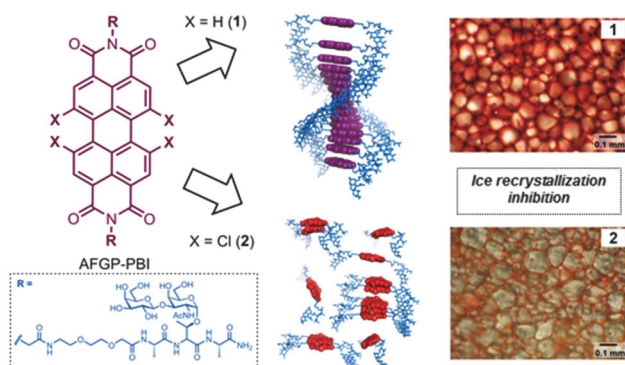
((Insert TOC Graphic here))

Page No. – Page No.

Title

Layout 2:

## COMMUNICATION



Page No. – Page No.

# 1D Self-assembly and Ice Recrystallization Inhibition Activity of Antifreeze Glycopeptide-functionalized Perylene bisimides

The synthesis, 1D self-assembly and ice recrystallization inhibition activity of antifreeze glycopeptide-functionalized perylene bisimides (AFGP-PBIs, **1** and **2**) is reported. AFGP-PBIs displayed variable aggregation behavior that depended on core substitution and were also shown to be weak inhibitors of ice recrystallization.